BIOCHEMISTRY
including biophysical chemistry & molecular biology

Article

pubs.acs.org/biochemistry

Amphitrite ornata Dehaloperoxidase (DHP): Investigations of Structural Factors That Influence the Mechanism of Halophenol Dehalogenation Using "Peroxidase-like" Myoglobin Mutants and "Myoglobin-like" DHP Mutants

Jing Du,[†] Xiao Huang,[†] Shengfang Sun,[†] Chunxue Wang,[†] Lukasz Lebioda,*[,†] and John H. Dawson*[,†,‡]

[†]Department of Chemistry and Biochemistry, University of South Carolina, Columbia, South Carolina 20208, United States

[‡]School of Medicine, University of South Carolina, Columbia, South Carolina 20208, United States

Supporting Information

ABSTRACT: Dehaloperoxidase (DHP), discovered in the marine terebellid polychaete *Amphitrite ornata*, is the first heme-containing globin with a peroxidase activity. The sequence and crystal structure of DHP argue that it evolved from an ancient O_2 transport and storage globin. Thus, DHP retains an oxygen carrier function but also has the ability to degrade halophenol toxicants in its living environment. Sperm whale myoglobin (Mb) in the ferric state has a peroxidase activity ~10 times lower than that of DHP. The catalytic activity enhancement observed in DHP appears to have been generated mainly by subtle changes in the positions of the proximal and distal histidine residues that appeared during DHP evolution. Herein, we report investigations into the mechanism of action of DHP derived from examination of "peroxidase-like" Mb mutants and "Mb-like" DHP mutants. The dehalogenation ability of wild-type Mb is augmented in the peroxidase-like Mb mutants (F43H/H64L, G65T, and G65I Mb) but attenuated in the Mb-like T56G DHP variant. X-ray crystallographic data show that the distal His residues in G65T Mb and G65I are positioned ~0.3 and ~0.8 Å, respectively, farther from the heme iron compared to that in the wild-type protein. The H93K/T95H double mutant Mb with the proximal His shifted to the "DHP-like" position has an increased peroxidase activity. In addition, a better dehaloperoxidase (M86E DHP) was generated by introducing a negative charge near His89 to enhance the imidazolate character of the proximal His. Finally, only minimal differences in dehalogenation activities are seen among the exogenous ligand-free DHP, the acetate-bound DHP, and the distal site blocker L100F DHP mutant. Thus, we conclude that binding of halophenols in the internal binding site (i.e., distal cavity) is not essential for catalysis. This work provides a foundation for a new structure−function paradigm for peroxidases and for the molecular evolution of the dual-function enzyme DHP.

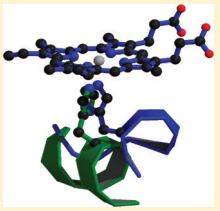

Halophenols are known to be harmful to mammalian liver and immune systems and have been listed as priority pollutants by the U.S. Environmental Protection Agency.[1] Furthermore, phenoxy radicals are able to modify DNA bases and have been classified as potential carcinogens.[2−4] The first peroxidase active heme-containing globin, dehaloperoxidase (DHP), was originally discovered from the coelom of the terebellid polychaete *Amphitrite ornata*.[5,6] The survivability of *A. ornata* in an environment contaminated with toxic haloaromatics extruded from organisms (such as *Notomastus lobatus*) that contain the necessary haloperoxidases for their synthesis is mainly attributed to the detoxifying physiological function of DHP. DHP catalyzes the hydrogen peroxide (H_2O_2)-dependent dehalogenation of a wide variety of mono-, di-, and trisubstituted halophenols to the corresponding quinone products (eq 1).[5,7,8] The H_2O_2-dependent oxidative dehalogenation reaction mechanism involves two consecutive one-electron steps via a phenoxy radical mediated by the high-valent oxidants Compound I (Cpd I) (Fe^{IV}=O porphyrin π-cation radical) or Compound II-Y$^{\bullet}$ (Cpd II-Y$^{\bullet}$) (Fe^{IV}=O with a tyrosyl radical) and Compound II (Cpd II) (Fe^{IV}=O state).[9,10]

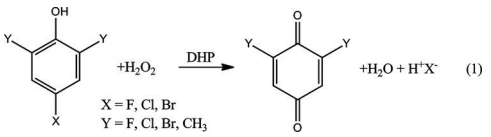

DHP is homodimeric with two heme iron-containing subunits of 15.5 kDa. Two genes encoding DHP were found; the predicted protein sequences are 97% identical.[11] The protein isolated from *A. ornata* appears to be predominantly DHP A.[12] Despite the relatively low degree of sequence homology between DHP and myoglobin (Mb), the two proteins have almost the same protein fold, with a root-mean-square distance between the positions of C^{α} atoms of 1.8 Å[12−16] (Figure 1A). The most significant deviation is at the proximal sites of DHP and Mb (Figure 1B) with the proximal His of DHP positioned in the sequence two residues farther toward the C-terminus than in Mb.[17] This distorts the α-helical structure of the peptide backbone to a coil conformation and

Received: June 13, 2011
Revised: July 28, 2011
Published: July 29, 2011

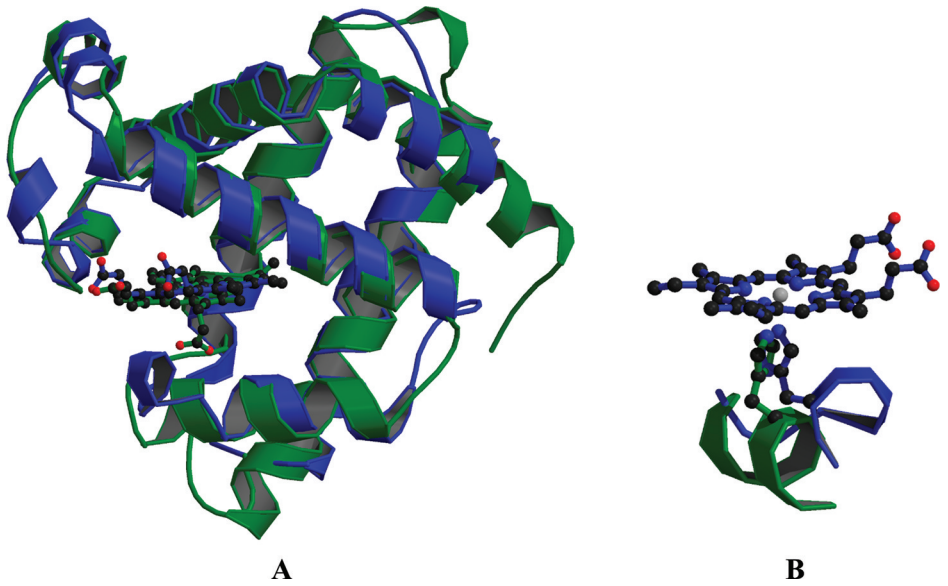

Figure 1. (A) DHP (blue, PDB entry 1EW6) and Mb (green, PDB entry 1A6K) are superposed on the basis of the positions of C^{α} atoms. (B) Relative positions of the proximal His in DHP and Mb. Only the DHP heme is shown. The main chain for the DHP His is in a coil conformation, while it is in the helical conformation in Mb. To be approximately in the same spatial position, the proximal His is shifted in the amino acid sequence by two residues, but the different conformation of the main chain results in the plane of the imidazole ring being rotated by ~60°.

causes the plane of the proximal His imidazole ring to rotate ~60° relative to that in Mb.

Typically, the ferric resting state of heme-containing peroxidases has a five-coordinate structure with the heme iron ligated by a partially deprotonated His. In the traditional "push−pull" mechanism for heme peroxidases, this proximal anionic His is thought to facilitate heterolytic O−O bond cleavage of bound peroxide to generate the ferryl Cpd I intermediate.[18,19] However, our initial spectroscopic studies revealed that ferric DHP, like ferric Mb, is a six-coordinate heme-containing enzyme bearing a neutral His as the proximal ligand to the heme iron and water on the distal side.[20,21] All the ferric-CN, deoxyferrous, ferrous-O_2, and ferrous-CO DHP derivatives spectroscopically resembled parallel states of Mb and were less similar to corresponding horseradish peroxidase derivatives.[22] Thus, the peroxidase activity of DHP does not arise from the push effect imparted by a partially ionized proximal His as proposed for typical heme-containing peroxidases in the classic push−pull paradigm.[18,19,23] Although heme-containing peroxidases usually oxidize organic substrates at the heme edge; the X-ray crystallography data revealed that an organic substrate (4-iodophenol) can bind in the distal cavity of DHP with the distal His55 swinging out of the cavity.[12,24,25] Recent investigations have determined that the dehalogenation activity for 2,4,6-tribromophenol is inhibited by 4-halophenols in the distal pocket of DHP. Thus, it has been proposed that ligand binding in the distal cavity of DHP is inhibitory and does not represent the binding site for the natural substrates.[24,25]

The increasing availability of genomic data shows that globin-based O_2 carrier proteins are universal and arose quite early in evolution.[26,27] In fact, DHP is isolated in the oxyferrous state after protein purification in the absence of any reductant,[20] while most heme-containing proteins, including peroxidases, are isolated in the ferric state.[28] This extraordinary fact indicates that DHP has unusual oxyferrous state stability. Sequence alignment data show that the N-terminal 28-amino acid sequence of *Enoplobranchus sanguineus* coelomic hemoglobin (physiological oxygen carrier) is 32% identical to that of DHP.[29] Our previous data demonstrate that physiological O_2 carrier horse heart Mb also catalyzes the H_2O_2-dependent oxidative dehalogenation of chlorophenols to the corresponding quinones.[30] The turnover of phenolic substrate oxidation by DHP is much faster than the reaction catalyzed by Mb, although it is more than 1 order of magnitude slower than with horseradish peroxidase.[7,30] It is quite likely that DHP has two functions in marine organisms, i.e., serving as both an O_2 carrier and an enzyme with dehaloperoxidase activity. We recently reported that the combination of substrate 2,4,6-trichlorophenol (TCP) and as little as one oxidation equivalent (0.5 molar equiv of H_2O_2) induced the functional switching of the O_2-carrying ferrous DHP to the peroxidase active ferric state, providing a physiological link for this bifunctional protein.[28] Thus, DHP apparently has evolved from an ancient oxygen carrier globin by acquiring mutations that enhanced its peroxidase activity.[12,28] However, the necessity of conducting double duties in *A. ornata* might preclude DHP from becoming a more efficient dehaloperoxidase.

We propose that the peroxidase activity of DHP arose mainly through the changes in the positions of the proximal and distal His residues compared to those in globins. It is likely that different protein dynamics amplify the peroxidase activity to yield the enhanced catalytic function. In this study, DHP and myoglobin mutants have been prepared and studied to explore the mechanistic role of individual vital amino acids near the DHP heme center. In particular, we find that Mb mutants designed to mimic the heme environment in DHP have appreciably enhanced dehaloperoxidase abilities. On the other hand, "Mb-like" DHP mutants are found to have diminished enzymatic reactivity.

Another major question in DHP catalysis is the actual binding site of organic substrates in this enzyme, i.e., the internal active site (the distal pocket) or the external one (the heme edge like most heme-containing peroxidases). Six-coordinate acetate-bound DHP as well as a distal site large side chain amino acid mutant (L100F DHP) was utilized in

dx.doi.org/10.1021/bi2009129 | *Biochemistry* 2011, 50, 8172–8180

Table 1A. Crystallographic Data

	G65T (PDB entry 3OCK)	G65I (PDB entry 3SDN)
heme ligand	water	acetate
X-ray source	LS CAT 21-ID-G	SER-CAT 22-ID
detector	MAR 300 CCD	Mar 300 CCD
wavelength (Å)	0.97856	1.00000
no. of frames, range	100, 1°	270, 0.5°
space group	*P*6	$P2_12_12_1$
unit cell dimensions (Å)		
a	90.50	40.04
b	90.50	48.01
c	45.25	77.56
resolution range (Å) (highest-resolution shell)	32.0−1.26 (1.11−1.09)	40.82−1.50 (1.53−1.50)
volume (Å^3)	320502	149080
redundancy (highest-resolution shell)	2.5 (1.5)	2.6 (1.5)
completeness (%) (highest-resolution shell)	90.1 (60.6)	87.1 (45.7)
total no. of reflections	168452	56050
no. of unique reflections	98403	24768
$I/\sigma(I)$	14.2 (2.0)	19.6 (6.7)
total linear R_{merge}	0.049 (0.411)	0.074 (0.222)

Table 1B. Crystallographic Refinement Parameters

	G65T (PDB entry 3OCK)	G65I (PDB entry 3SDN)
refinement software	SHELXL	Refmac5
resolution (highest-resolution shell)	48−1.09 (1.09−1.13)	40−1.50 (1.53−1.50)
R	0.152 for all 82924 data	0.177; 0.206[a] for all 20386 data
R_{free}	0.180 for 4358 data	0.238; 0.250[a] for 1102 data
R for $F > 4\sigma(F)$	0.132 for 64546 data	
R_{free} for $F > 4\sigma(F)$	0.159 for 3387 data	
R in the highest-resolution shell	0.312	0.186 (0.299)
root-mean-square deviation from ideal values [bonds (Å); angles (deg)]	0.015	0.024; 2.0
average *B* factor (Å^2) for protein	10.2	20.3
average *B* factor (Å^2) for solvent	41.8	39.2
residues with most favored ϕ and ψ (%)	93.5	97.3
residues in additionally allowed regions (%)	6.5	2.7

[a] *R* factor values for isotropic *B* refinement.

kinetic studies to exclude the possibility of halophenol substrate binding to the internal distal pocket. Those results demonstrate that substrate binding in the distal cavity is not an essential prerequisite for dehalogenation catalysis by DHP.

EXPERIMENTAL PROCEDURES

Reagents. All reagents and biochemicals were purchased from Aldrich, ACROS, or Fisher and used without further purification except for potassium ferricyanide, which was recrystallized from water.

Mutagenesis and Sample Preparation. The pET 16b plasmid containing the DNA of six-His-tagged DHP A was transformed into BL21(DE3) *Escherichia coli* competent cells. The expression vectors (pUC 19) for wild-type and F43H/H64L sperm whale Mb were gifts from Y. Watanabe (Nagoya University, Nagoya, Japan). Sperm whale Mb mutants (pUC 19-G65T, -G65I, and -H93K/T95H) and DHP mutants (pET 16b-T56G, -M86E, and -L100F) were all produced by the QuickChange method. All mutations were verified by LiCor DNA sequence analysis of the entire Mb gene (Engencore at the University of South Carolina). Six-His-tagged DHPs were expressed and purified as previously described.[8,28,31] His-tagged DHP exhibits the same enzymatic activity as recombinant DHP for oxidizing the substrate TCP.[8] Mbs were expressed in *E. coli* strain BL21(DE3) in this study, and purification was performed as described previously.[32−34] The isolated Mb and DHP exist mostly in the oxyferrous states. Complete oxidation of the heme iron is accomplished by addition of a few crystals of potassium ferricyanide (Fluka) followed by gel-filtration column chromatography in 100 mM potassium phosphate buffer (pH 5) at 4 °C.

Protein concentrations were determined by the pyridine hemochromogen method (ε_{555} = 34.4 M^{-1} cm^{-1})[35] and are the concentrations of the heme component. The H_2O_2 stock (10 mM) in deionized water was prepared daily from a 30% stock solution, and H_2O_2 concentrations were confirmed spectrophotometrically (ε_{240} = 39.4 M^{-1} cm^{-1}). 2,4,6-TCP stocks (10 mM) were freshly made in a 50:50 ethanol/deionized water mixture.

Peroxidase Activity Assay. UV absorption spectroscopy was used to measure the peroxidase activity of the wild-type enzyme and mutants (0.1−10 μM enzyme). Hydrogen peroxide was used to initiate the reactions in a 0.5 cm cuvette. The turnover number was measured by monitoring the change in absorbance at 272 nm for the appearance of quinone products (ε_{272} = 12 mM^{-1} cm^{-1}) as a function of time.[36] The turnover number was determined by calculating the velocity from the initial linear portion of the trace at 272 nm as a function of H_2O_2 concentration (0−6.4 mM). For each set of

reaction conditions, 10 individual reactions were performed and then averaged to determine the velocity at the varying H_2O_2 concentrations. For measuring the turnover number at pH 5.4, 50 mM sodium acetate buffer was used for Mb (Mb forms are almost inactive in 50 mM sodium citrate buffer at pH 5.4) and 50 mM sodium citrate buffer for DHPs. All pH 7.0 studies were conducted in 100 mM potassium phosphate buffer.

Crystallization. Crystals of G65T Mb were grown by the vapor diffusion method using the hanging-drop setup under conditions similar to those reported previously.[32] Briefly, 50 mM Tris-HCl (pH 8.5), 2.6−2.8 M ammonium sulfate, and 1.0 mM EDTA were used. The native and soaked G65T crystals were flash-cooled in N_2 vapor at 100 K. Crystals of G65I Mb were grown by the vapor diffusion method using the hanging-drop setup under different conditions [0.1 M PIPES (pH 6.5), 0.3 M sodium acetate, 0.1% dioxane, and 32−36% PEG 8000]. The native and soaked G65I crystals were flash-cooled in N_2 vapor at 100 K.

X-ray Diffraction Data Collection and Structure Determination. Data were collected on the LS CAT 21-ID-G and SER-CAT 22-ID beamlines at Argonne National Laboratory and processed with HKL2000.[37] Data collection and processing statistics are listed in Table 1A. The structures were determined using molecular replacement with AMoRe[38] from the CCP4 suite of programs[39] using the sperm whale Mb structure (PDB entry 1H1X) as the starting model. Structure rebuilding and subsequent refinements were performed using Turbo-Frodo,[40] WinCoot,[41] and SHELXL.[42] The final refinements were conducted using Refmac5.[43] Superpositions were calculated using LSQKAB[44] from the CCP4 suite of programs. Figure 1 was created using MOLSCRIPT[45] and Raster3D.[46] Figure 2 was prepared using Turbo-Frodo. *R* factors of the final models are listed in Table 1A along with data collection and other refinement statistics (Table 1B).

Acetate Binding to the Distal Site of DHP. Acetate binding studies were conducted at pH 7.0 in 100 mM potassium phosphate buffer at 4 °C. Binding of acetate to DHP was monitored by measuring changes in the absorption spectrum in the Soret and visible regions using a Cary 400 spectrophotometer. For each titration, ligand was added in a small increment to a single protein solution and absorbance changes were monitored to ensure that equilibrium was reached after each addition.

Determining the Binding Affinity of the Organic Substrate TCP for DHP. TCP was added in small increments to a DHP protein solution, and absorbance changes were monitored with a Cary 400 spectrophotometer by ensuring that equilibrium was reached after each addition. Titration studies were conducted at 4 °C in 100 mM potassium phosphate buffer (pH 5 and 7.0).

MCD and UV−vis Absorption Spectroscopic Investigation. UV−visible (UV−vis) absorption spectra were recorded on a Cary 400 spectrophotometer interfaced with a Dell computer. Magnetic circular dichroism (MCD) spectra were measured with a magnetic field strength of 1.41 T using a JASCO J815 spectropolarimeter equipped with a JASCO MCD 1B electromagnet and interfaced with a Silicon Solutions personal computer through a JASCO IF-600-2 interface unit. Data acquisition and manipulation were conducted as described previously.[47] UV−vis absorption spectra were recorded before and after the MCD measurements to confirm the integrity of the samples.

RESULTS AND DISCUSSION

As the first discovered heme-containing globin carrying peroxidase activity, DHP has a fold that is very similar to that of Mb.[12,13] We have demonstrated that horse heart Mb also catalyzes the H_2O_2-dependent oxidative dehalogenation of TCP to the corresponding dichloroquinone at a relatively low reaction rate.[30] However, the unique structural properties of DHP challenge the traditional standard push−pull paradigm for the mechanism of heme-containing peroxidase activity.[18,19] In this study, we propose that the much higher peroxidase activity of DHP relative to Mb mainly arises from subtle changes in the positions and orientations of specific residues (i.e., proximal His and distal His) adjacent to the heme iron center.

Altering the Position of the Distal His: Mb-like T56G DHP Mutant and "Peroxidase-like" F43H/H64L, G65T, and G65I Mb Mutants. The position of the distal His in DHP relative to the heme iron is close to the range of positions seen for the distal His in various peroxidases, so that it can exert its essential function as an acid−base catalyst for the activation of bound peroxide to form the Cpd I intermediate.[34] As previously described in the standard push−pull model, the proper distances between the heme iron and the proximal and distal histidine residues are essential to the typical peroxidase activity. On the basis of the available crystal structures, the distances between the $N^{\varepsilon 2}$ atom of the distal His and the heme iron in globins are usually between 4.1 and 4.6 Å (4.3 Å for sperm whale Mb), whereas this distance increases to 5.5−6.0 Å in heme-containing peroxidases.[12,34] For DHP, this distance is 5.4 Å.[12] Comparing the relevant amino acid sequence of DHP with Mb (Scheme S1 of the Supporting Information), the amino acid adjacent to the distal His is Gly65 in Mb, which corresponds to Thr56 in DHP. Gly65 is almost completely conserved in globins having a distal His. It appears that the increase in the His $N^{\varepsilon 2}$−heme iron distance in DHP is generated by replacing Gly65 in Mb with Thr56 in DHP. The larger Thr side chain induces a shift in the position of the distal His C^{α} and might increase the distal His−heme iron distance. Indeed, the interactions of larger side chains of residue 65 in G65T and G65I with the α-helix push the main chain away from the heme iron. As a result of this push, the C^{α} positions of neighboring His64 are shifted 0.3 and 0.8 Å from the position of C^{α} in wild-type Mb (*wt*-Mb) in G65T and G65I, respectively, while distances between the C^{α} and Fe atoms are 8.6, 8.7, and 8.9 Å in *wt*-Mb, G65T, and G65I, respectively. For our analysis of peroxidase activity, these distances should be more significant than the distances between $N^{\varepsilon 2}$ and Fe atoms for two reasons. First, the experimental error in C^{α} coordinates should be smaller because of stronger restraints; second, the side chain−imidazole moiety may adjust its position to bind a different Fe ligand (water in *wt*-Mb and G65T and acetate in G65I).

When the distal ligand is the same, the $N^{\varepsilon 2}$ of His64 forms a hydrogen bond with the water molecule coordinated to the Fe in *wt*-Mb (2.7 Å) and G65T (3.0 Å). The significant difference in the length of this bond is likely due to the restriction imposed by the position of the main chain and reflects the strength of this interaction. The weaker bonding of the water/hydroxide coordinated to Fe must facilitate its replacement by peroxide and contributes to the higher peroxidase activity. Similarly, in aquomet-DHP (PDB entry 2QFK), the hydrogen bond between the water molecule and the distal histidine is fairly long, 3.1 Å. In the G65I·acetate complex, a short distance,

2.6 Å, between the acetate oxygen atom that is not coordinated to Fe and the $N^{\varepsilon 2}$ atom of His64 indicates the formation of a strong hydrogen bond and thus histidine protonation, which must contribute to the inhibition of peroxidase activity by acetate (see below).

The Watanabe double mutant, F43H/H64L of sperm whale Mb, was designed to increase the distance between the distal His and heme iron center and yielded a much higher peroxidase activity with standard peroxidase substrates compared to that of *wt*-Mb.[34] The crystal structure confirmed that the distal His in F43H/H64L Mb is a similar distance (5.4 Å) from the heme iron as observed in peroxidases.[34] In this study, the peroxidase-like activity of F43H/H64L sperm whale Mb is utilized as a benchmark Mb mutant and compared to the activity of G65T and G65I variants of Mb. On the other hand, the T56G DHP mutant was generated to mimic the distal site environment of Mb. It should be pointed out that in the F43H/H64L mutant the replacement of distal His (His64) alters the "gate" to the distal cavity; this is not the case in G65 mutants.

Figure S1 of the Supporting Information shows the MCD and UV−vis absorption spectra of wild-type, G65T, and G65I Mb. The overall spectral patterns of G65T and G65I Mb mutants are very similar to those of the wild-type protein. The UV−vis spectroscopic data for protein samples are summarized in Table 2. For the G65T and G65I Mb mutants, their Soret

Table 2. UV−Vis Absorption Spectroscopic Data for Sperm Whale Mbs and DHPs at pH 7

	λ_{max} (nm)		
	Soret	visible	ref
wt-Mb	408	502, 632	30
G65T Mb	409	504, 632	this work
G65I Mb	409	504, 632	this work
H93K/T95H Mb	409	500, 536, 574, 625	this work
F43H/H64L Mb	407	502, 630	31
T56G DHP	408	521, 633	this work
wt-DHP	407	504, 538, 576, 634	22
M86E DHP	413	534, 576, 626	this work
L100F DHP	407	502, 534, 574, 630	this work

peaks are all at 409 nm and the two visible bands are around 504 and 632 nm, indicating the mutants folded properly and there is no significant change in the heme environment. Turnover numbers (k_{cat}) for the dechlorination of TCP are listed in Table 3. Wild-type Mb has the lowest activities at both pH 5.4 (optimal pH for peroxidase activity) and pH 7 (coelomic physiological pH). DHP has a much higher turnover number than Mb, especially at pH 5.4. As expected, the dehaloperoxidase activities of the standard peroxidase-like F43H/H64L Mb mutant are greatly enhanced at both pH values compared to those of the wild-type enzyme. The G65T Mb mutant shows 3−5 times higher peroxidase activity than *wt*-Mb. Its structure indicates that the distance between the distal His64 and the heme iron is ~4.6 Å (Figure 2). This distance is ~0.3 Å longer than that of *wt*-Mb, while other amino acids in the active site remain in approximately the same positions. The G65I Mb mutant has been constructed to push the peptide chain further and widen the distance between the distal His and the heme iron. The design worked well, and the dehalogenation activity was further increased as a result of the G65I mutation (Table 3 and Figure 2). The crystal structure showed indeed an increase in the His−heme iron distance.

Table 3. Turnover Numbers for the Oxidative Dechlorination with Enzyme, 150 μM TCP, and Varying H_2O_2 Concentrations in 50 mM Sodium Citrate Buffer (pH 5.4) (DHPs) or 50 mM Sodium Acetate Buffer (pH 5.4) (Mbs) and 100 mM Potassium Phosphate Buffer (pH 7) at 4 °C

protein (ferric state) at 4 °C		k_{cat} [mol of product (mol of enzyme)$^{-1}$ min^{-1}]		Fe−N(His) distance (Å)
		pH 5.4	pH 7.0	
wt-Mb		18.7 ± 1.7	2.8 ± 0.1	4.3
G65T Mb	HRP-like[a]	92.2 ± 7.0	10.6 ± 2.4	4.6
H93K/T95H Mb	DHP-like[a]	104 ± 13	12.7 ± 2.0	–
G65I Mb	HRP-like[a]	138 ± 10	129 ± 10	5.1
F43H/H64L Mb	HRP-like[a]	161 ± 9	48.8 ± 2.4	5.4
T56G DHP	Mb-like[a]	91.5 ± 13.6	75.4 ± 5.5	–
wt-DHP		243 ± 3	7.9 ± 0.3	5.4
M86E DHP	HRP-like[a]	349 ± 21	72.6 ± 5.1	–
L100F DHP	blocked distal pocket	180 ± 15	6.0 ± 0.1	–

[a]The specific mutation has been designed to mimic the active site properties of the protein listed.

In contrast, the oxidative dehalogenation activity for "myoglobin-like" T56G DHP variant decreases ~2.6-fold at pH 5.4. However, the kinetic turnover number for this DHP mutant is increased at pH 7 (Table 3). Further study shows that T56G DHP has only ~20% of the enzymatic efficiency (k_{cat}/K_m) of the wild type under the same conditions (data not shown). The MCD and UV−vis absorption spectra indicate that T56G DHP has more low-spin character with its Soret absorption peak at 408 nm and charge transfer (CT) bands at 521 and 633 nm (Figure S2 of the Supporting Information and Table 2). The optimal pH value for peroxidase activity is in the acidic range (≈5). A plausible explanation for the inconsistent turnover number change in T56G DHP at different pH values may be that the rate-limiting step of the dehalogenation reaction at pH 7 is less dependent on the distance between distal His and heme iron. The compromised DHP activity of the T56G DHP mutant and the opposite effect of the G65T Mb mutant indicate that Thr56 in DHP is essential for keeping the distal His in the precise position, which is similar to the case for peroxidases rather than globins.

Modifying the Position of the Proximal His, Peroxidase-like H93K/T95H Mb Mutants. Figure 1B shows the relative positions of the proximal His in DHP and Mb obtained by superimposing their structures. The proximal His in DHP is positioned in the sequence two residues farther toward the C-terminus than it is in myoglobins. The structures of this protein fragment are quite different. In particular, for DHP, the proximal His is in a coil conformation, whereas for Mb, it is in an α-helical conformation. An H93K/T95H Mb double mutant was prepared to place the proximal His in approximately the same spatial position as in DHP by moving the proximal His by two residues in the amino acid sequence toward the C-terminus. Unfortunately, the yield of the mutant was low, and we could not crystallize it. Its model based on the DHP structure indicates that the plane of the imidazole ring of the proximal His in this double mutant will rotate ~60° because of the different conformation of the main chain (data not shown).

The MCD and UV−vis absorption spectra of H93K/T95H are displayed in Figure S3 of the Supporting Information.

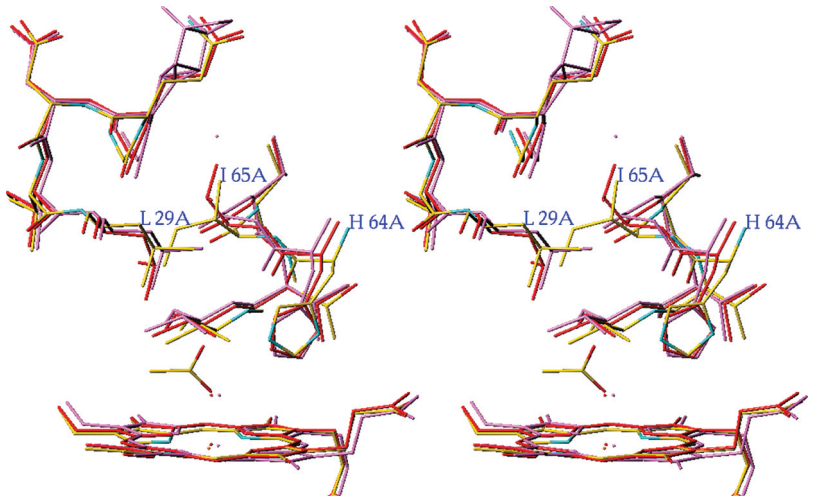

Figure 2. Stereoview of the distal cavity of wild-type aquomet-Mb (PDB entry 1A6K) (purple), G65T (red), and G65I (atom colors). The superposition of the structures is based on the positions of C^{α} atoms of residues 1−152. The side chain conformations of threonine and isoleucine in position 65 are quite different because of the limited space available in the cavity. The distal ligand is an acetate ion in G65I and a water molecule in the two other structures.

Compared to wild-type Mb, this double mutant has a weaker Soret peak at 409 nm and four visible bands at 500, 536, 574, and 625 nm. It is noted that the resulting spectra are similar to those of wild-type DHP (Table 2). Moreover, this double mutation increases the Mb peroxidase activity by ∼5-fold at pH 5.4 as well as pH 7 (Table 3). The enhanced activity of the DHP-like H93K/T95H Mb double mutant strongly suggests that the shift in the location of the proximal His residue and the precise rotational position of the imidazole ring play important roles in the increased dehaloperoxidase activity of DHP relative to that of wild-type Mb.

Introducing Negative Charge near the Proximal His: Peroxidase-like M86E DHP. With respect to the classic push−pull paradigm for peroxidase activity,[17,21] most heme-containing peroxidases have a partially deprotonated proximal His ("push effect") that works in concert with a nonligated distal His as an H^+ acceptor/donor as well as a cationic Arg to stabilize developing negative charge ("pull effect") during O−O bond cleavage.[17−19,21] However, DHP lacks the negatively charged amino acid (Asp) in the proximal side. We noticed that Met86 in DHP is close to the proximal His. By replacing Met with Glu, we have introduced a negative charge near the proximal His89. Theoretically, this surrogate should mimic typical peroxidases in generating a stronger imidazolate push and perhaps make DHP a faster peroxidase.

The MCD and UV−vis absorption spectra of heme centers are sensitive to heme iron coordination. In comparison with that of wild-type DHP, the Soret absorption peak of M86E DHP is red-shifted to 413 nm with visible region maxima at 534, 576, and 626 nm (Figure S4 of the Supporting Information). The spectral features indicate that the heme iron center of M86E DHP is in mostly a low-spin state. As shown in Table 3, the turnover number for the dehaloperoxidase activity of the M86E DHP mutant is increased at both pH 5.4 and 7. This suggests that a more active peroxidase enzyme has been engineered by enhancing the imidazolate character of the proximal His.

Acetate Binding in the Distal Cavity of Ferric DHP Monitored by UV−Vis Absorption. Franzen and co-workers have recently suggested that studies of the oxidative dehalogenation by DHP at acidic pH should be conducted in citrate buffer, because acetate buffers caused the loss of heme from ferric DHP.[48] As shown in Figure S5 of the Supporting Information, ferric *wt*-DHP exhibits a UV−vis absorption spectrum with a Soret peak at 406 nm and CT band at ∼633 nm in 50 mM sodium citrate buffer (pH 5.4) at 4 °C. We find that the turnover number for DHP in sodium citrate buffer (Table S1 of the Supporting Information) at the same pH is only slightly (approximately 1.2-fold) higher than the value in acetate buffer previously reported by Osborne et al.[7] Furthermore, stepwise addition of acetate to ferric DHP in citrate buffer produces an increase in the Soret absorption maximum and a blue shift of the charge transfer band (Figure S5 of the Supporting Information). There is a clear set of isosbestic points for the spectral conversion as the acetate concentration is increased during the titration. This indicates that throughout the acetate titration, there are two optically distinct heme ligation states: exogenous ligand-free and acetate-bound ferric DHP. The sample was very stable, and there was no indication of heme loss during the titration. The titration data have been analyzed by using a hyperbolic saturation plot (Figure S6 of the Supporting Information). Maximal absorbance changes in difference spectra (data not shown) [ΔA_{λ_1} or $\Delta A_{\lambda_1} - \Delta A_{\lambda_2}$, where λ_1 and λ_2 are wavelengths at which maximal positive (peak) and negative (trough) absorbance changes are observed, respectively] in the Soret region are plotted as a function of total ligand concentration. Lines drawn are nonlinear fits for a bimolecular association model to the data. The dissociation constant of acetate binding to ferric *wt*-DHP is 0.94 mM. The resulting MCD and UV−vis absorption spectra (Figure S7 of the Supporting Information) of the ferric acetate complex resemble those of the ferric *wt*-Mb acetate or formate complex with acetate or formate as the distal ligand, respectively.

Thus, we conclude that acetate ion binds in the distal cavity to the heme iron of ferric DHP. Citrate ion is much larger than acetate ion, so it cannot enter the distal pocket of DHP. The slightly lower peroxidase activity of DHP in acetate buffer compared to that in citrate buffer can be explained by the competition between acetate and peroxide (H_2O_2) for binding

dx.doi.org/10.1021/bi2009129|*Biochemistry* 2011, 50, 8172−8180

in the distal site (a prerequisite for Cpd I formation) instead of the previously reported heme loss problem.[48]

Determination of the Substrate TCP Binding Position: L100F DHP Mutant. A major remaining question in DHP catalysis is whether the enzyme binds substrates in the distal cavity (internal binding site) or if the reaction proceeds at the heme edge (external active site) like typical heme-containing peroxidases. It has been shown by X-ray crystallography that the substrate 4-iodophenol binds in the distal pocket above the heme plane of DHP.[12] The Franzen group has recently reported that binding in this site favored by 4-halophenols is inhibitory, while trisubstituted substrates like TCP bind in an external active site.[24,25] Nonetheless, the location of the binding site for the TCP substrate is still in question in the absence of direct structural evidence.

To further explore this issue, we replaced Leu100 with a larger side chain amino acid residue. The C^{δ} atoms of Leu100 form 4.1 and 4.5 Å contacts with the I atom of 4-iodophenol.[12] Modeling indicated that the larger side chain of Phe in position 100 can be accommodated in the cavity but would push out the iodophenol molecule ~1.2 Å (Figure S8 of the Supporting Information). On the other hand, the mutation should not interfere with peroxide binding. We hypothesized that if the binding of halophenols in the distal cavity is essential for catalysis, the mutant will have severely attenuated DHP activity. If TCP binds to an external position (such as the heme edge) and catalysis does not require substrate binding in the distal cavity, then the dehalogenation activity should be similar to that of wild-type DHP. Leu100 is fairly strongly conserved in myoglobins. The MCD and UV−vis absorption spectra of ferric L100F DHP are similar to those of wild-type DHP (Figure S9 of the Supporting Information), except the slight increase in the intensity of the two CT bands around 532 and 574 nm. The spectra indicate that the mutant folds properly and mutation does not interfere with the coordination of the heme iron center. Kinetic results demonstrate that there is no large difference in the turnover numbers between the L100F DHP mutant and wild-type enzyme at both pH 5.4 and 7 (Table 3). The results of this study further confirm that binding of halophenol substrates in the distal cavity is not required for the dehalogenation activity of DHP. This is consistent with the proposal that the mechanism of DHP involves reaction at the external active site most likely at the heme edge, like the majority of other heme-containing peroxidases.[49]

Substrate TCP Binding to Ferric DHP Monitored by UV−Vis Absorption Spectra. The absorption spectra reported previously show that TCP has a minimal effect on the spectra of the ferric protein based on the similar intensity and position of the Soret peak for DHP in the presence and absence of substrate TCP.[10] Although the change is small, in this study we report that the absorption spectra of ferric DHP are altered, especially in the Soret region, upon TCP titration in 50 mM citrate buffer (pH 5.4) at 4 °C (Figure S10 of the Supporting Information). In particular, the intensity of the Soret peak slightly increases following TCP addition. The dissociation constant (K_d) for binding of TCP to ferric DHP is 51.0 μM (Figure S11 of the Supporting Information). However, at TCP concentrations of >150 μM, the resulting spectra lost their isosbestic points. This indicates that DHP activity might be limited if the TCP concentration is too much higher than the physiological level. A similar TCP titration experiment was conducted with the ferric L100F DHP mutant (Figure S12 of the Supporting Information). The dissociation constant for binding of TCP to ferric L100F DHP is ~89.0 μM (Figure S13 of the Supporting Information), indicating that the binding affinity of TCP for L100F DHP is slightly weaker compared to that of the wild-type enzyme. Although the titration data can be analyzed to reveal a binding constant, the minimal extent of spectral change is more consistent with the weak influence of the substrate on the heme iron as would be expected for binding to an external binding site such as the heme edge rather than direct binding to the heme iron in the distal site. Consequently, these results also suggest that substrate binding in the distal cavity is not a prerequisite for the dehalogenation function. Considering the small changes in absorption spectra of TCP titration to both ferric DHP and L100F mutant, substrate TCP could bind to an external position (like heme edge) and catalyze the H_2O_2-dependent dehalogenation function.

CONCLUSIONS

DHP is a dual-function globin or, to be more precise, an oxidation state-dependent alternate function protein. Its structure and amino acid sequence indicate that it evolved from an oxygen carrier and acquired dehaloperoxidase function. The close structural relationship to other globins indicates that DHP represents a very early stage of the emergence of a new function in molecular evolution. The characterization of a series of mutants has allowed us to dissect how this new function was acquired and at the same time to identify the significance of different structural factors in peroxidase catalysis.

As the first globin-shaped dehalogenation peroxidase, DHP challenges the current push−pull paradigm of how peroxidases function. The neutral His-ligated DHP has retained its ability to bind O_2 and is isolated in the oxyferrous state, ready to convert to the peroxidase active ferric enzyme in the presence of substrate TCP and a stoichiometric amount of H_2O_2.[28] It is apparent that DHP is a dual-function protein, detoxifying halophenols present in the *A. ornata* environment as well as continuing to be a physiological O_2 carrier. In this study, we have demonstrated that subtle changes in the positions of the proximal and distal His of Mb and DHP mutants induce different enzymatic activities. The peroxidase-like Mb mutants show appreciably enhanced dehaloperoxidase abilities, whereas the Mb-like DHP mutant has attenuated enzymatic reactivity. It is also likely that different protein dynamics (movement of distal His55) can amplify the peroxidase activity to yield a greater activity.

L100F DHP, the mutant excluding the halophenol substrate binding in the distal pocket, exhibited an only slightly smaller binding affinity for TCP as well as enzymatic activity comparable to that of the wild-type enzyme. These results further confirmed the proposal that physiological substrates bind to DHP at the heme edge like most heme-containing peroxidases. This study has probed how nature has redesigned small Mb-like proteins to convert them into a catalytic peroxidase and has extended the boundaries of our current understanding of structure−mechanism relationships in dual-function proteins.

ASSOCIATED CONTENT

Supporting Information

Alignment of Mb and DHP amino acid sequences (Scheme S1), MCD and absorption spectra of DHP and Mb mutants (Figures S1−S4, S7, and S9), titrations of DHP and its mutants with acetate and TCP (Figures S5, S6, and S10−S13),

modeling of the DHP L100F mutant (Figure F8), and DHP inhibition by acetate (Table S1). This material is available free of charge via the Internet at http://pubs.acs.org.

Accession Codes

‡Crystal coordinates for G65T and G65I variants of sperm whale myoglobin mutants have been deposited in the Protein Data Bank as entries 3OCK and 3SDN, respectively.

AUTHOR INFORMATION

Corresponding Author

*Department of Chemistry and Biochemistry, University of South Carolina, 631 Sumter St., Columbia, SC 29208. Phone: (803) 777-2414 or (803) 777-7234. Fax: (803) 777-9521. E-mail: lebioda@mail.chem.sc.edu (L.L.) or dawson@sc.edu (J.H.D.).

Author Contributions

J.D. and X.H. contributed equally to this work.

Funding

Financial support provided by the National Science Foundation (MCB 0820456).

ACKNOWLEDGMENTS

We thank Prof. David P. Ballou (University of Michigan, Ann Arbor, MI) and Dr. Masanori Sono (University of South Carolina) for helpful discussions, Prof. Stefan Franzen (North Carolina State University, Raleigh, NC) for the six-His-tagged DHP plasmid, and Professor Yoshi Watanabe (Nagoya University) for the F43H/H64L Mb plasmid. Data were collected at the SER-CAT 22-ID and 22-BM beamlines at the Advanced Photon Source, Argonne National Laboratory. Use of the Advanced Photon Source was supported by the U.S. Department of Energy, Office of Basic Energy Sciences, under Contract W-31-109-Eng-38.

ABBREVIATIONS

DHP, dehaloperoxidase; Cpd I, Compound I; Cpd II, Compound II; Cpd II-Y$^{\bullet}$, Compound II-Y$^{\bullet}$; Mb, sperm whale myoglobin; TCP, 2,4,6-trichlorophenol; UV−vis, UV−visible; MCD, magnetic circular dichroism; K_d, dissociation constant; PDB, Protein Data Bank.

REFERENCES

(1) Pera-Titus, M., Garcia-Molina, V., Banos, M. A., Gimenez, J., and Esplugas, S. (2004) Degradation of chlorophenols by means of advanced oxidation processes: A general review. *Appl. Catal., B 47*, 219−256.

(2) Dix, T. A., and Aikens, J. (1993) Mechanisms and Biological Relevance of Lipid-peroxidation Initiation. *Chem. Res. Toxicol. 6*, 2−18.

(3) Stadtman, E. R. (1992) Protein oxidation and aging. *Science 257*, 1220−1224.

(4) Burrows, C. J., and Muller, J. G. (1998) Oxidative nucleobase modifications leading to strand scission. *Chem. Rev. 98*, 1109−1151.

(5) Chen, Y. P., Woodin, S. A., Lincoln, D. E., and Lovell, C. R. (1996) An unusual dehalogenating peroxidase from the marine terebellid polychaete *Amphitrite ornata*. *J. Biol. Chem. 271*, 4609−4612.

(6) Zhang, E., Chen, Y. P., Roach, M. P., Lincoln, D. E., Lovell, C. R., Woodin, S. A., Dawson, J. H., and Lebioda, L. (1996) Crystallization and initial spectroscopic characterization of the heme-containing dehaloperoxidase from the marine polychaete *Amphitrite ornata*. *Acta Crystallogr. D52*, 1191−1193.

(7) Osborne, R. L., Taylor, L. O., Han, K. P., Ely, B., and Dawson, J. H. (2004) *Amphitrite ornata* dehaloperoxidase: enhanced activity for the catalytically active globin using MCPBA. *Biochem. Biophys. Res. Commun. 324*, 1194−1198.

(8) Belyea, J., Gilvey, L. B., Davis, M. F., Godek, M., Sit, T. L., Lommel, S. A., and Franzen, S. (2005) Enzyme function of the globin dehaloperoxidase from *Amphitrite ornata* is activated by substrate binding. *Biochemistry 44*, 15637−15644.

(9) Osborne, R. L., Coggins, M. K., Raner, G. M., Walla, M., and Dawson, J. H. (2009) The mechanism of oxidative halophenol dehalogenation by *Amphitrite ornata* dehaloperoxidase is initiated by H_2O_2 binding and involves two consecutive one-electron steps: Role of ferryl intermediates. *Biochemistry 48*, 4231−4238.

(10) Feducia, J., Dumarieh, R., Gilvey, L. B. G., Smirnova, T., Franzen, S., and Ghiladi, R. A. (2009) Characterization of dehaloperoxidase compound ES and its reactivity with trihalophenols. *Biochemistry 48*, 995−1005.

(11) Han, K., Woodin, S. A., Lincoln, D. E., Fielman, K. T., and Ely, B. (2001) *Amphitrite ornata*, a marine worm, contains two dehaloperoxidase genes. *Mar. Biotechnol. 3*, 287−292.

(12) LaCount, M. W., Zhang, E. L., Chen, Y. P., Han, K. P., Whitton, M. M., Lincoln, D. E., Woodin, S. A., and Lebioda, L. (2000) The crystal structure and amino acid sequence of dehaloperoxidase from *Amphitrite ornata* indicate common ancestry with globins. *J. Biol. Chem. 275*, 18712−18716.

(13) Lebioda, L., LaCount, M. W., Zhang, E. L., Chen, Y. P., Han, K. P., Whitton, M. M., Lincoln, D. E., and Woodin, S. A. (1999) An enzymatic globin from a marine worm. *Nature 401*, 445−445.

(14) D'Antonio, J., D'Antonio, E. L., Thompson, M. K., Bowden, E. F., Franzen, S., Smirnova, T., and Ghiladi, R. A. (2010) Spectroscopic and mechanistic investigations of dehaloperoxidase B from *Amphitrite ornata*. *Biochemistry 49*, 6600−6616.

(15) Franzen, S., Belyea, J., Gilvey, L. B., Davis, M. F., Chaudhary, C. E., Sit, T. L., and Lommel, S. A. (2006) Proximal cavity, distal histidine, and substrate hydrogen-bonding mutations modulate the activity of *Amphitrite ornata* dehaloperoxidase. *Biochemistry 45*, 9085−9094.

(16) Vojtechovsky, J., Chu, K., Berendzen, J., Sweet, R. M., and Schlichting, I. (1999) Crystal structures of myoglobin-ligand complexes at near-atomic resolution. *Biophys. J. 77*, 2153−2174.

(17) Lebioda, L. (2000) The honorary enzyme haemoglobin turns out to be a real enzyme. *Cell. Mol. Life Sci. 57*, 1817−1819.

(18) Poulos, T. L., and Kraut, J. (1980) The stereochemistry of peroxidase catalysis. *J. Biol. Chem. 255*, 8199−8205.

(19) Dawson, J. H. (1988) Probing structure-function relations in heme-containing oxygenases and peroxidases. *Science 240*, 433−439.

(20) Roach, M. P., Chen, Y. P., Woodin, S. A., Lincoln, D. E., Lovell, C. R., and Dawson, J. H. (1997) *Notomastus lobatus* chloroperoxidase and *Amphitrite ornata* dehaloperoxidase both contain histidine as their proximal heme iron ligand. *Biochemistry 36*, 2197−2202.

(21) Franzen, S., Roach, M. P., Chen, Y.-P., Dyer, R. B., Woodruff, W. H., and Dawson, J. H. (1998) The unusual reactivities of *Amphitrite ornata* dehaloperoxidase and *Notomastus lobatus* chloroperoxidase do not arise from a histidine imidazolate proximal heme iron ligand. *J. Am. Chem. Soc. 120*, 4658−4661.

(22) Osborne, R. L., Sumithran, S., Coggins, M. K., Chen, Y. P., Lincoln, D. E., and Dawson, J. H. (2006) Spectroscopic characterization of the ferric states of *Amphitrite ornata* dehaloperoxidase and *Notomastus lobatus* chloroperoxidase: His-ligated peroxidases with globin-like proximal and distal properties. *J. Inorg. Biochem. 100*, 1100−1108.

(23) Poulos, T. L. (1996) The role of the proximal ligand in heme enzymes. *J. Biol. Inorg. Chem. 1*, 356−359.

(24) Davis, M. F., Bobay, B. G., and Franzen, S. (2010) Determination of separate inhibitor and substrate binding sites in the dehaloperoxidase-hemoglobin from *Amphitrite ornata*. *Biochemistry 49*, 1199−1206.

(25) Thompson, M. K., Davis, M. F., de Serrano, V., Nicoletti, F. P., Howes, B. D., Smulevich, G., and Franzen, S. (2010) Internal binding of halogenated phenols in dehaloperoxidase-hemoglobin inhibits peroxidase function. *Biophys. J. 99*, 1586−1595.

(26) Moens, L., Vanfleteren, J., Van de Peer, Y., Peeters, K., Kapp, O., Czeluzniak, J., Goodman, M., Blaxter, M., and Vinogradov, S.

(1996) Globins in nonvertebrate species: Dispersal by horizontal gene transfer and evolution of the structure-function relationships. *Mol. Biol. Evol. 13*, 324−333.
(27) Vinogradov, S. N., Hoogewijs, D., Bailly, X., Arredondo-Peter, R., Guertin, M., Gough, J., Dewilde, S., Moens, L., and Vanfleteren, J. R. (2005) Three globin lineages belonging to two structural classes in genomes from the three kingdoms of life. *Proc. Natl. Acad. Sci. U.S.A. 102*, 11385−11389.
(28) Du, J., Sono, M., and Dawson, J. H. (2010) Functional switching of *Amphitrite ornata* dehaloperoxidase from O_2-binding globin to peroxidase enzyme facilitated by halophenol substrate and H_2O_2. *Biochemistry 49*, 6064−6069.
(29) Weber, R. E., Mangum, C., Steinman, H., Bonaventura, C., Sullivan, B., and Bonaventura, J. (1977) Hemoglobins of two terebellid polychaetes: *Enoplobranchus sanguineus* and *Amphitrite ornata*. *Comp. Biochem. Physiol., Part A: Mol. Integr. Physiol. 56*, 179−187.
(30) Osborne, R. L., Coggins, M. K., Walla, M., and Dawson, J. H. (2007) Horse heart myoglobin catalyzes the H_2O_2-dependent oxidative dehalogenation of chlorophenols to DNA-binding radicals and quinones. *Biochemistry 46*, 9823−9829.
(31) Davis, M. F., Gracz, H., Vendeix, F. A. P., de Serrano, V., Somasundaram, A., Decatur, S. M., and Franzen, S. (2009) Different modes of binding of mono-, di-, and trihalogenated phenols to the hemoglobin dehaloperoxidase from *Amphitrite ornata*. *Biochemistry 48*, 2164−2172.
(32) Springer, B. A., Egeberg, K. D., Sligar, S. G., Rohlfs, R. J., Mathews, A. J., and Olson, J. S. (1989) Discrimination between oxygen and carbon monoxide and inhibition of autooxidation by myoglobin. Site-directed mutagenesis of the distal histidine. *J. Biol. Chem. 264*, 3057−3060.
(33) Springer, B. A., and Sligar, S. G. (1987) High-level expression of sperm whale myoglobin in *Escherichia coli*. *Proc. Natl. Acad. Sci. U.S.A. 84*, 8961−8965.
(34) Matsui, T., Ozaki, S., Liong, E., Phillips, G. N. Jr., and Watanabe, Y. (1999) Effects of the location of distal histidine in the reaction of myoglobin with hydrogen peroxide. *J. Biol. Chem. 274*, 2838−2844.
(35) Paul, K. G., Theorell, H., and Akeson, A. (1953) The molar light absorption of pyridine ferroprotoporphyrin (pyridine hemochromogen). *Acta Chem. Scand. 7*, 1284−1287.
(36) Oberg, L. G., and Paul, K. G. (1985) The transformation of chlorophenols by lactoperoxidase. *Biochim. Biophys. Acta 842*, 30−38.
(37) Otwinowski, Z., and Minor, W. (1997) Processing of X-ray diffraction data collected in oscillation mode. *Methods Enzymol. 276*, 307−326.
(38) Navaza, J. (1994) AMoRe: An automated package for molecular replacement. *Acta Crystallogr. D50*, 157−163.
(39) Collaborative Computational Project, Number 4 (1994) The CCP4 suite: Programs for protein crystallography. *Acta Crystallogr. D50*, 760−763.
(40) Roussel, A., and Cambillau, C. (1991) Turbo Frodo Silicon Graphics Geometry Partners Directory, p 86, Silicon Graphics, Mountain View,CA.
(41) Emsley, P., Lohkamp, B., Scott, W. G., and Cowtan, K. (2010) Features and development of Coot. *Acta Crystallogr. D66*, 468−501.
(42) Sheldrick, G. M., and Schneider, T. R. (1997) SHELXL: High resolution refinement. *Methods Enzymol. 277*, 319−343.
(43) Murshudov, G. N., Vagin, A. A, and Dodson, E. J. (1997) Refinement of macromolecular structures by the maximum-likelihood method. *Acta Crystallogr. D53*, 240−255.
(44) Kabsch, W. (1976) A solution for the best rotation to relate two sets of vectors. *Acta Crystallogr. A32*, 922−923.
(45) Kraulis, P. J. (1991) MOLSCRIPT: A program to produce both detailed and schematic plots of protein structures. *J. Appl. Crystallogr. 24*, 946−950.
(46) Merritt, E. A., and Bacon, D. J. (1997) Raster3D: Photorealistic molecular graphics. *Methods Enzymol. 277*, 505−524.
(47) Pond, A. E., Roach, M. P., Sono, M., Huff, A., Franzen, S., Hu, R., Thomas, M. R., Wilks, A., Dou, Y., Ikeda-Saito, M., Ortiz de Montellano, P. R., Woodruff, W. H., Boxer, S. G., and Dawson, J. H. (1999) Assignment of the heme axial ligand(s) for the ferric myoglobin (H93G) and heme oxygenase (H25A) cavity mutants as oxygen donors using magnetic circular dichroism. *Biochemistry 38*, 7601−7608.
(48) Franzen, S., Gilvey, L. B., and Belyea, J. L. (2007) The pH dependence of the activity of dehaloperoxidase from *Amphitrite ornata*. *Biochim. Biophys. Acta 1774*, 121−130.
(49) Poulos, T. L. (2010) Thirty years of heme peroxidase structural biology. *Arch. Biochem. Biophys. 500*, 3−12.